

---

## North Atlantic palaeointensity stack since 75ka (NAPIS –75) and the duration of the Laschamp event

Carlo Laj, Catherine Kissel, Alain Mazaud, James E. T. Channell and Juerg Beer

*Phil. Trans. R. Soc. Lond. A* 2000 **358**, 1009-1025

doi: 10.1098/rsta.2000.0571

---

### Email alerting service

Receive free email alerts when new articles cite this article - sign up in the box at the top right-hand corner of the article or click [here](#)

---

To subscribe to *Phil. Trans. R. Soc. Lond. A* go to:  
<http://rsta.royalsocietypublishing.org/subscriptions>

---

# North Atlantic palaeointensity stack since 75 ka (NAPIS-75) and the duration of the Laschamp event

BY CARLO LAJ<sup>1</sup>, CATHERINE KISSEL<sup>1</sup>, ALAIN MAZAUD<sup>1</sup>,  
JAMES E. T. CHANNELL<sup>2</sup> AND JUERG BEER<sup>3</sup>

<sup>1</sup>*Laboratoire des Sciences du Climat et de l'Environnement, CEA-CNRS,  
Avenue de la Terrasse, Bat. 12, 91198, Gif-sur-Yvette Cedex, France*

<sup>2</sup>*Department of Geological Sciences, University of Florida, PO Box 112120,  
Gainesville, FL 32611-2120, USA*

<sup>3</sup>*Environmental Physics, Swiss Federal Institute of Science and Technology,  
CH-8600 Dübendorf, Switzerland*

Six relative palaeointensity records from the north Atlantic Ocean were stacked together to produce a new record for the last 75 kyr (NAPIS-75). Five of these records have been previously correlated at millennial scale and placed on the GISP2 age scale, the sixth record was tied to the others using magnetic susceptibility. From 75 ka the field strength exhibits some oscillations, with a first minimum *ca.* 65 ka, followed by a progressive increase to a broad maximum centred at *ca.* 48 ka. There is then a well-marked low at 40 ka, corresponding to the directional anomaly of the Laschamp event. Another intensity low, observed at *ca.* 34 ka, corresponds in age to the Mono Lake event. After a high at 33 ka and two lows at 30 and 24 ka with a broad maximum between, the field strength seems to slowly increase to the upper limit of the studied interval. In the 10–20 kyr interval some differences exist between individual records, and fine-scale details are not always resolved. In the 20–75 kyr interval, on the other hand, well-resolved millennial-scale features are superimposed to the broader trends. The duration of the Laschamp event, which is recorded directionally in five cores, appears to be about 1500 years, consistent with a recent suggestion on the origin of geomagnetic excursions.

**Keywords:** palaeomagnetism; correlation; geomagnetic events; Atlantic Ocean

## 1. Introduction

Study of geomagnetic field intensity recorded in marine sediments, in time and space, has two principal objectives: firstly, to understand the origin of palaeointensity variations in terms of the geodynamo and, secondly, to assess the potential of geomagnetic intensity variations as a mean of stratigraphic correlation (see, for example, Peck *et al.* 1996). The Sint-200 (Guyodo & Valet 1996) and more recently the Sint-800 (Guyodo & Valet 1999) palaeointensity stacks, based respectively on 17 and 33 globally distributed palaeointensity records, have demonstrated the global synchronism of long wavelength ( $10^4$ – $10^5$  kyr) features in the individual records. Shorter wavelength features are not apparent in these two stacks because of the low sedimentation rates

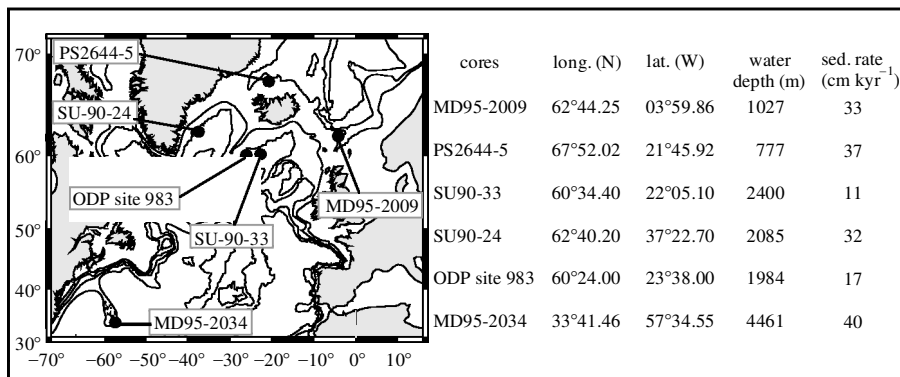


Figure 1. Schematic map of the north Atlantic Ocean showing the location of the studied cores and the bathymetry (1000 m contour interval). The latitude and longitude of each site are reported with the water depths and the average sedimentation rate.

of individual records and the smoothing effect of stacking records with imperfect chronologies.

Recent coring of high deposition rate ‘drift’ deposits in the North Atlantic has led to the determination of a number of palaeointensity records from sediments with sedimentation rates in excess of 10 cm kyr<sup>-1</sup>. Some authors have suggested that palaeointensity records may provide a powerful high-resolution method for global-scale correlation (see, for example, Peck *et al.* 1996; Stoner *et al.* 1995); however, some authors believe that variable amplitude and number of individual features limit the usefulness of palaeointensity records as a means of high-resolution correlation (Schwartz *et al.* 1998).

Here we report new relative palaeointensity records for the 10–75 ka interval from six North Atlantic cores separated by as much as 5000 km, all of which are characterized by mean sedimentation rates of at least 10 cm kyr<sup>-1</sup>. These records are combined to produce a palaeointensity stack (NAPIS-75) for the 10–75 ka period. For this limited time-interval, millennial-scale correlation among cores with high sedimentation rate results in a very detailed relative palaeointensity stack with well-defined short-wavelength features.

Although NAPIS-75 is derived from the North Atlantic region only, it shows striking similarity with other records from the Blake Outer Ridge, with high-resolution records from outside of the North Atlantic and with the long-wavelength features of Sint-200. Moreover, correlation with cosmogenic isotope production, as recorded in the GRIP ice core, implies that the millennial-scale variability is a fundamental feature of the global scale geomagnetic field. This geomagnetic record, in addition, gives a precise estimate of the duration of the Laschamp event, both directionally and in intensity.

## 2. Previous work

The location of the cores is shown schematically in figure 1. Five cores were collected between 58° N and 67° N and from 45° W to 4° E at different water depths, while the sixth was sampled at a lower latitude (33° N). They are all located in areas known for their high mean sedimentation rates (10–20 cm kyr<sup>-1</sup>). The SU90 cores were collected

during the PALEOCINAT-I cruise of the RV *Le Suroit* in 1990, while the MD95 cores were recovered in 1995 during the IMAGES-I cruise of RV *Marion Dufresne* (Bassinot & Labeyrie 1996). Core PS2644-5 was obtained by the RV *Polar Stern*. Site 983 was drilled during Ocean Drilling Program (ODP) Leg 162. A description of these cores is given in Kissel *et al.* (1999, and references therein), Channell *et al.* (1997) and Voelker *et al.* (1998).

Previous work has shown that the magnetic mineralogy is virtually identical in the different cores and is dominated by low-Ti-content magnetite with uniform grain sizes in the pseudo-single-domain range (Kissel *et al.* 1999). The bulk magnetic parameters of all these cores exhibit short-term variations which reflect small changes in the relative amount of the magnetic fraction within the detrital fraction, linked to changes in the strength of the bottom current (Kissel *et al.* 1999). Previous work on the ODP Site 983 has also established that the magnetic mineralogy is suitable for relative palaeointensity determinations over this interval (Channell *et al.* 1997).

A precise millennial-scale correlation has been established between five of these cores for marine isotopic stage (MIS) 3 (27–60 ka) (Kissel *et al.* 1999). This correlation uses identification of detrital (Heinrich) layers and Ash layer 2 in the first step, then the record of short-lived oscillations in the magnetic susceptibility and anhysteretic remanent magnetization in the second step. Furthermore, using the correlation established by Voelker *et al.* (1998) between the planktic  $\delta^{18}\text{O}$  record of core PS2644-5 and the  $\delta^{18}\text{O}$  record of the GISP2 ice core (Grootes & Stuiver 1997), all the data have been placed on the GISP2 age model.

### 3. Methods

The six cores have been subsampled continuously using *u*-channels (Tauxe *et al.* 1983; Weeks *et al.* 1993). The natural remanent magnetization (NRM), the anhysteretic remanent magnetization (ARM) and the isothermal remanent magnetization (IRM) were measured with a pass-through high-resolution DC-SQUIDS cryogenic magnetometer in the shielded room of the LSCE. Stepwise in-line alternating-field (AF) demagnetization was used with an average of 8–10 steps. ARM was imparted along the axis of the *u*-channel using a 100 mT AF and 50  $\mu\text{T}$  DC field. IRM was acquired along the *Y*-axis of the *u*-channel by passing it through the poles of an electromagnet. Low-field susceptibility was measured every centimetre on the *u*-channels using a Bartington loop sensor with a 45 mm diameter. Analyses of the hysteresis parameters at 2.5–10 cm intervals downcore were performed using an alternating gradient force magnetometer (AGFM 2900). Thermomagnetic analyses were conducted at a few representative depths in each core.

### 4. Results

#### (a) Additional mineral magnetic studies

For the five cores which had been previously examined only for the MIS3 (Kissel *et al.* 1999) we have extended the mineral magnetic studies through the 10–75 ka interval. There are virtually no changes in the magnetic mineralogy over this longer period with respect to the shorter interval considered by Kissel *et al.* (1999). For all cores, the *S*-ratio (King & Channell 1991) values are close to unity with occasional

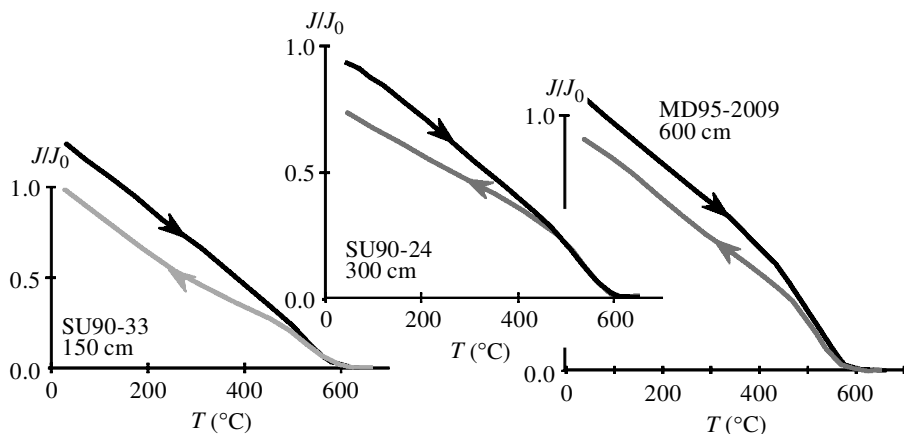


Figure 2. Representative high-field thermomagnetic curves showing a single Curie point at *ca.* 580 °C.

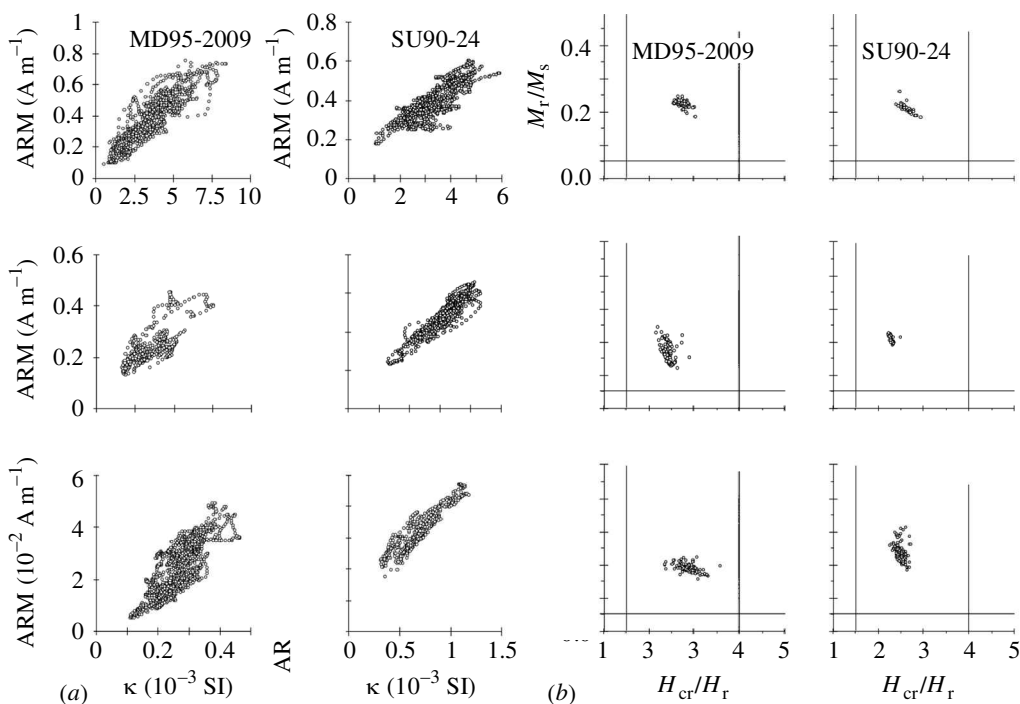


Figure 3. Grain-size indicators for magnetite: (a) ARM versus  $\kappa$  plots (Banerjee *et al.* 1981); (b) ‘Day’ plots (Day *et al.* 1977).

rapid excursions to values never lower than 0.85. This is consistent with a low-coercivity magnetic mineralogy. Curie-balance analyses of sediment samples from the different cores indicate that the magnetic mineralogy is dominated by low-Ti magnetite (figure 2). Isolated small black patches at the very top of the studied interval in core MD95-2034 (which could only be sampled from 15 m downward because of coring disturbance in the upper part) indicate localized precipitation of

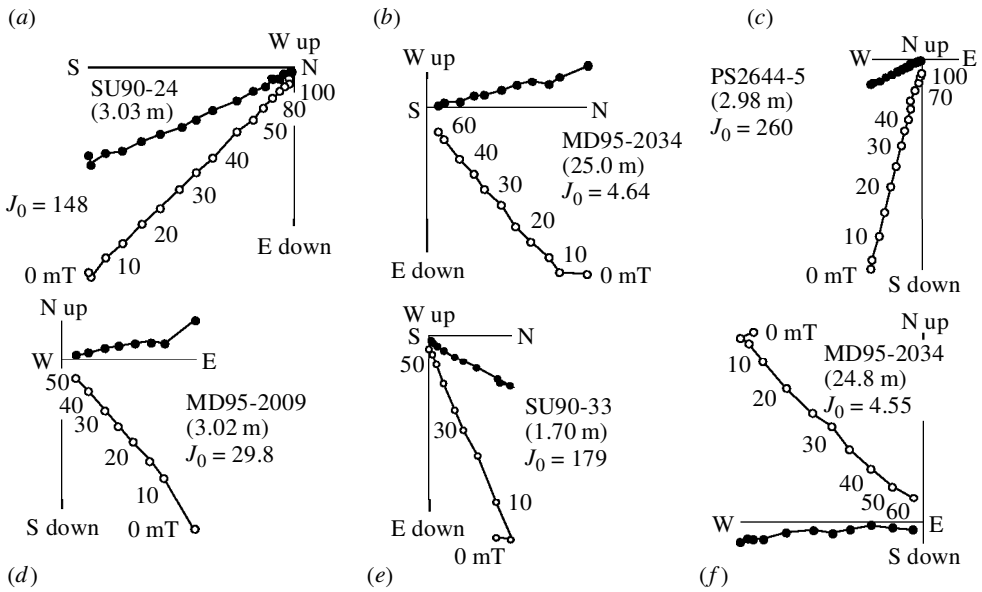


Figure 4. Representative AF demagnetization diagrams obtained from *u*-channel samples. The filled and open circles correspond to projections onto the horizontal and vertical planes, respectively.  $J_0$  is the magnetization intensity before demagnetization (units:  $10^{-3} \text{ A m}^{-1}$ ). The meter level (below sea floor) of the sample is indicated.

iron monosulphide (M. Cremer 1996, personal communication). An oxidized zone is present between 3.5 and 5 m depth at Site 983 (Channell *et al.* 1997) and between 32.5 and 35 m in core MD95-2034.

Plots of ARM versus volume susceptibility ( $\kappa$ ) are shown in figure 3*a*. In four of the cores, tight grouping of the points along a line emanating from the origin of the plot is consistent with very uniform magnetic grain size (Banerjee *et al.* 1981; King *et al.* 1982, 1983). For core MD95-2034, the line does not extrapolate through the origin, indicating that there is a significant paramagnetic contribution to the low field susceptibility. Hysteresis ratios, reported in the Day diagrams (Day *et al.* 1977) of figure 3*b*, tightly cluster within the pseudo-single domain (PSD) area, supporting the ARM- $\kappa$  results. Changes in ARM and  $\kappa$  also indicate that the concentration of magnetic grains in the sediments varies by at most a factor of eight. These results indicate that the criteria for relative palaeointensity estimates (see, for example, King *et al.* 1983) are satisfied in these North Atlantic sediments.

### (b) Extension of the correlation to the 10–75 kyr period and to ODP Site 983

Correlation between cores was carried out for the 10–75 ka interval using an approach similar to the two-step approach used for the MIS3 interval by Kissel *et al.* (1999). Firstly, isotopic stage boundaries 5/4, 4/3 and 2/1 and detrital (Heinrich) layer signals were used as tie points. Then, short-lived oscillations of the magnetic susceptibility were used to refine this correlation. These were, however, not quite as clear over the entire interval as in MIS3. For core MD95-2034 and ODP Site 983, the correlation could not be made for sediments younger than 20 and 15 ka, respectively. For all other cores, 10 ka was the young age limit for which correlation was possible.

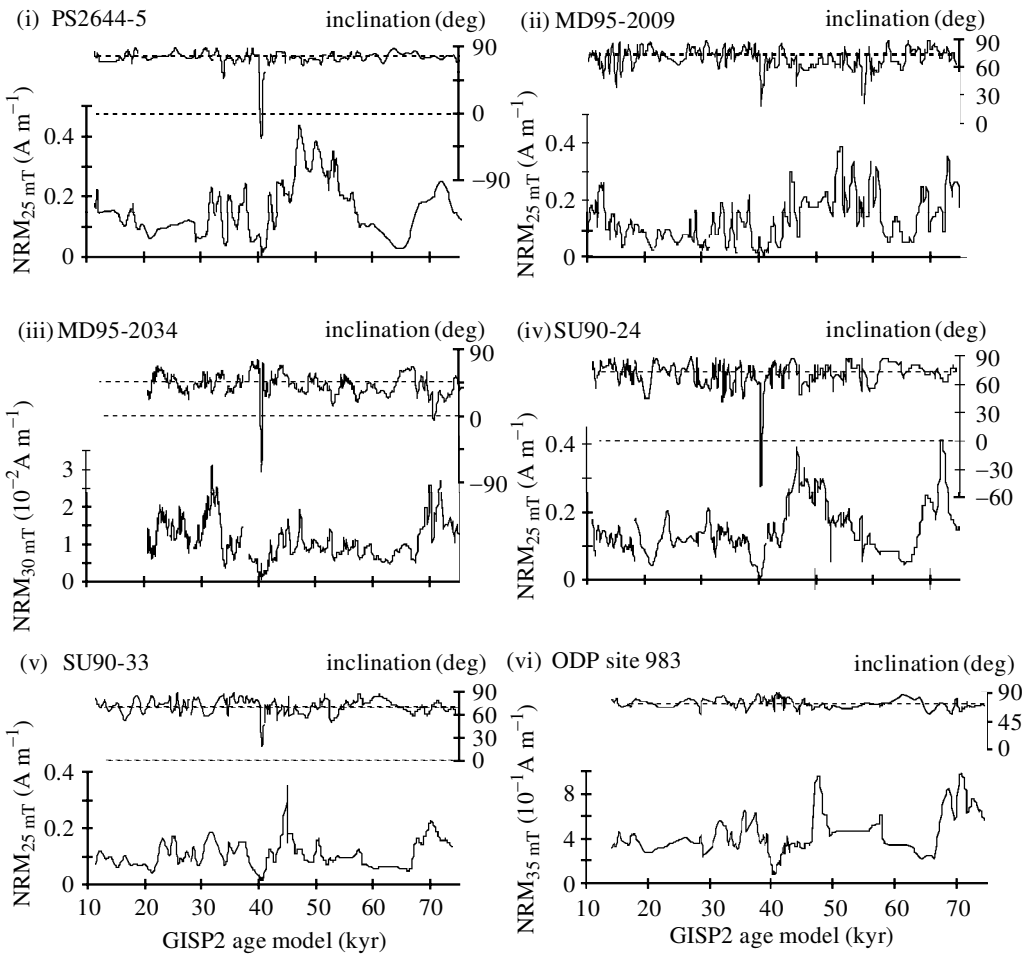


Figure 5. Records of inclination derived from principal component analysis and NRM intensity after demagnetization at 25 or 30 mT versus age.

All the cores have been correlated down to 75 ka and correlated to the GISP2 ice core age, allowing the GISP2 age model to be adopted.

### (c) Natural remanent magnetization

NRM component directions were calculated every 5 cm by generating orthogonal demagnetization plots, some of which are shown in figure 4. A single stable component of magnetization passing through the origin of the orthogonal projection was isolated at peak AF-fields of 20–25 mT using standard least-squares analysis. Maximum angular deviation (MAD) angles smaller than  $5^\circ$  for the great majority of cases indicate that NRM directions were precisely determined.

The inclinations derived from principal component analysis (PCA) and NRM intensity records of all the cores are given in figure 5. Inclinations fluctuate around the values expected for an axial geocentric dipole field at the different sites, and with a variability appropriate for geomagnetic secular variation. In five of the records a



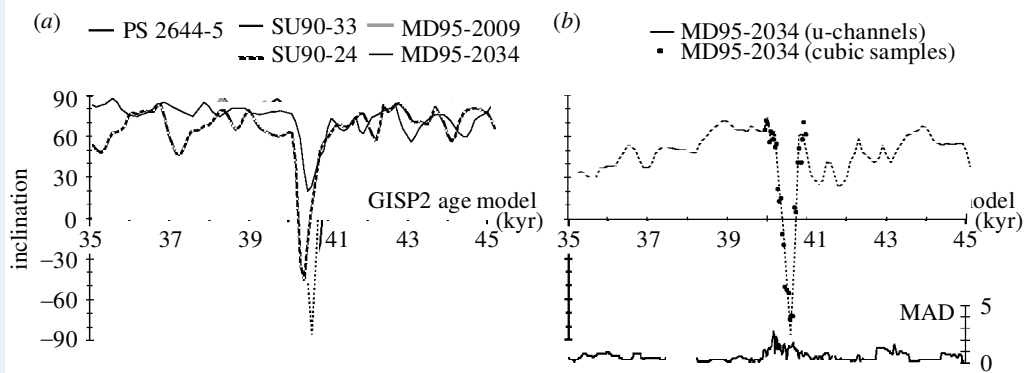


Figure 6. (a) Component inclination records from the five cores which have recorded the Laschamp event and (b) comparison between component inclinations obtained using the *u*-channel technique and the component inclinations obtained from cubic samples (black dots) for core MD95-2034. Values of the maximum angular deviation (MAD) are also reported.

A large inclination swing identified as the Laschamp event is recorded at *ca.* 40 ka. As shown in the enlarged view of figure 6a, the swing has different amplitudes in the different cores, probably reflecting different, but in all cases slight, degrees of smoothing. In the two more northerly cores (PS2644-5 and SU90-24), negative inclinations with maximum values *ca.*  $-45^\circ$  are observed. In the other two cores (SU90-33 and MD95-2009) very shallow positive inclinations are observed. Inclination reaches  $-90^\circ$  for the southernmost record (MD95-2034), implying that smoothing is very slight in this core. This last result has been confirmed (figure 6b) using standard  $2 \times 2 \times 2 \text{ cm}^3$  discrete samples, to ascertain that no perturbation has been introduced by the *u*-channel technique, in connection with the large intensity drop related to the Laschamp event (see Weeks *et al.* 1993). During this excursion, MAD values are similar to those observed outside this interval, as shown by the demagnetization diagrams relative to a reverse direction (figure 4f) and by figure 6b.

The important result is that the directional changes of the Laschamp event are recorded over a very short time-interval. There are offsets in the timing of the event in the different cores but they are very slight and reach a maximum of less than 500 years between cores SU90-24 and PS2644-5. They may be due either to small errors in the correlation of the cores or, more realistically, to slight differences in the magnetization lock-in depth in the different cores. These slight differences do not, however, significantly affect the determination of the duration of the directional changes of the Laschamp event which is about 1000 years in every case (figure 6). The duration of the event (in direction) is estimated from the time for which the inclination lies outside the normal range of secular variation.

#### (d) Normalized record of magnetization

Following Levi & Banerjee (1976) and King *et al.* (1982), ARM has been used as the normalizer to obtain records of normalized remanence. Very similar results were obtained using IRM or  $\kappa$  as normalizers (figure 7). The normalized records were generated using values of NRM and ARM after AF demagnetization at 25 mT, this peak field being sufficient for complete removal of secondary components present in



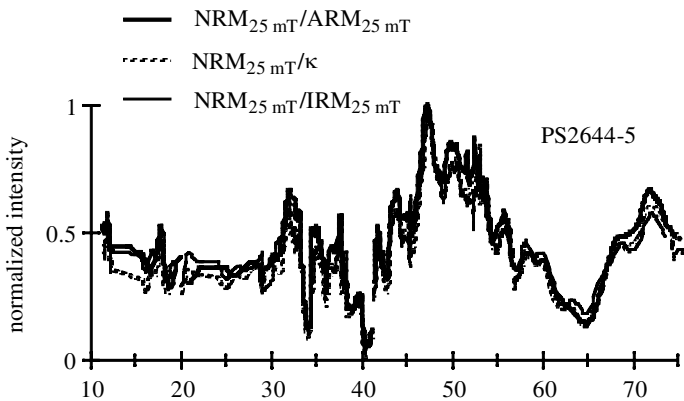


Figure 7. Comparison of palaeointensity profiles obtained using different normalizers (ARM, IRM and  $\kappa$ ) for core PS2644-5.

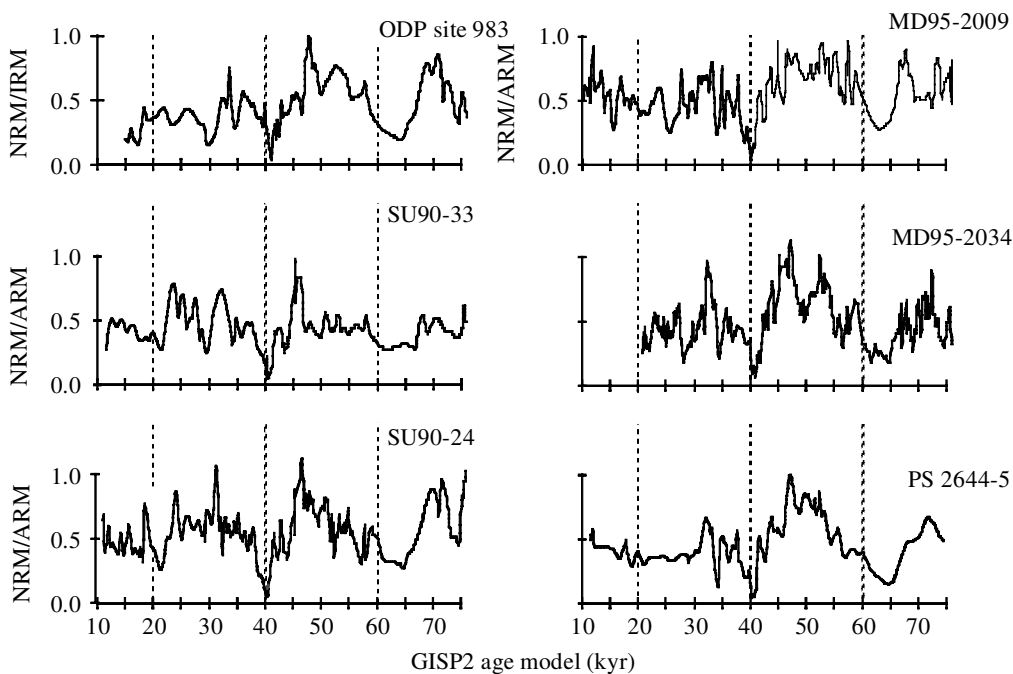


Figure 8. Individual records of normalized field intensity versus age obtained for the six cores.

the NRM. For ODP Site 983, we have used the IRM normalized record given by the authors (Channell *et al.* 1997).

Similarities among the six normalized records are illustrated in figure 8. Not only the broad long-term characteristics, but also short-lived features, appear to be recorded synchronously in the six records. To construct the stack, the six normalized records were first interpolated to a common sampling interval of 100 years (corresponding to *ca.* 1–2 cm) to give equal weight to each record in the stack. They were then scaled to obtain a common palaeointensity value for the minimum at *ca.* 40 ka,

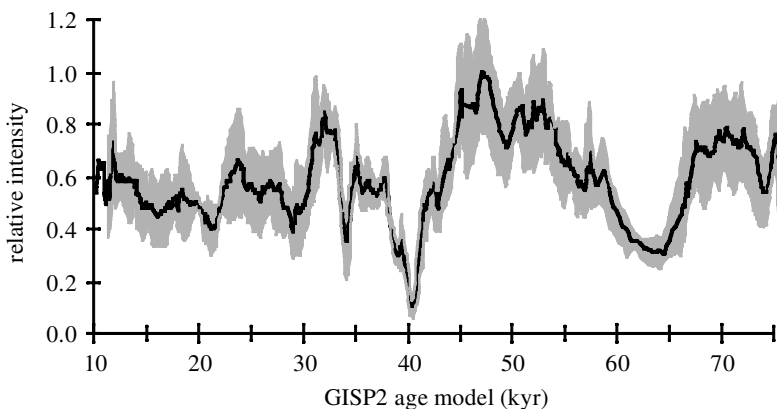


Figure 9. Stacked NAPIS-75 record obtained from the six studied cores. The shaded area corresponds to the  $\pm 2\sigma$  incertitude derived from the bootstrap calculation.

corresponding to the Laschamp event, and also to obtain a common average value in the (10–75 kyr) interval. This technique has the advantage of not being overly sensitive to abrupt variations in individual records. The stack was then determined using the arithmetic mean at each common interpolated sampling point.

The resulting stack is shown in figure 9 with associated uncertainties. Following Tauxe *et al.* (1991) the confidence limits were assessed using a bootstrap approach: ‘pseudo-samples’ were obtained by randomly drawing series of six records from the original records (each record may appear several times in a given pseudo-sample). Consistent with the recommendation of Hall (1988) we have used  $n^2$  pseudo-samples (here  $n^2 = 6 \times 6 = 36$ ) to ensure that the distribution of mean records is correctly represented. The  $\pm 2\sigma$  incertitude derived from this bootstrap calculation is shown as a grey shaded area in figure 9. In addition, we have also used a jackknife approach (see Caceci 1989) in which each individual record is in turn excluded from trial stacks. The departure of each trial stack from the mean value of the stack yields the estimate of standard deviation. The incertitudes calculated using the two approaches are almost identical.

As a consequence of the high degree of internal consistency between individual records (figure 8), the six stacks of five cores obtained from the jackknife approach are almost identical, and each individual record is very similar to the stack itself (figure 10) except for a small difference observed for core SU90-33 in the 45–50 kyr interval. High internal consistency is also indicated by values of the correlation coefficients between the stack and individual records, all of which are large and none departs from the average value (0.76) by more than  $2\sigma$  (table 1). The maximum discrepancy is observed for core SU90-33 which also has the lowest correlation coefficient (0.61).

## 5. Discussion

### (a) North Atlantic palaeointensity stack for the 10–75 ka interval (NAPIS-75)

Before assuming that the stacked record represents variations of the geomagnetic field, one must ascertain that it is not significantly affected by environmental factors.

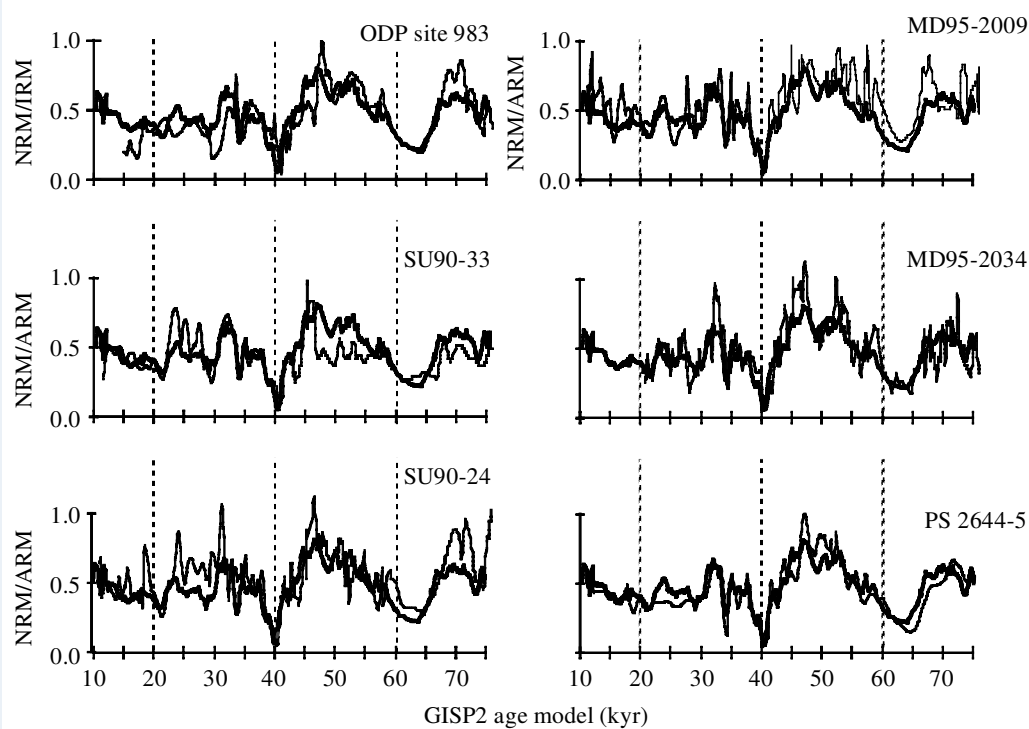


Figure 10. Stacked record NAPIS-75 superimposed on the individual records showing their internal consistency.

Table 1. Correlation coefficient between NAPIS-75 and the individual palaeointensity records

cores	coeff. correl.
NAPIS – PS2644-5	0.832
NAPIS – MD95-2009	0.766
NAPIS – SU90-33	0.611
NAPIS – ODP Site 983	0.812
NAPIS – SU90-24	0.731
NAPIS – MD95-2034	0.831

With this in mind, we have calculated the power (Blackman–Tukey) spectrum of the stacked record (figure 11a). Most of the power is distributed in a broad band  $ca. 0.2 \text{ kyr}^{-1}$  ( $T = 5 \text{ kyr}$ ) where it exceeds a 95% confidence level calculated from the first-order autoregressive process (red-noise generator). This spectrum is very different from those of bulk parameters of individual cores, such as ARM, of the individual records which document a peak at  $ca. 0.7 \text{ kyr}^{-1}$  ( $T = 1.4 \text{ kyr}$ ) related to Dansgaard–Oeschger climatic oscillations.

We have also calculated the coherence in the frequency domain between the normalized intensity and the environmental sensitive susceptibility of the different cores (figure 11b). Coherence slightly above the 95% confidence level is occasionally observed, particularly at relatively high frequencies. Frequencies at which coherence

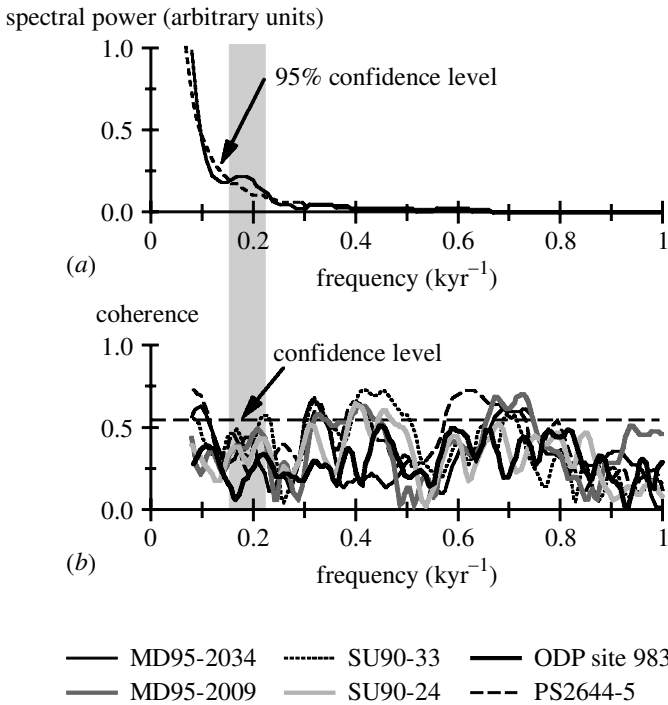


Figure 11. (a) Power spectrum of the stacked record showing a significant broad power peak at frequencies *ca.*  $0.2 \text{ kyr}^{-1}$ . (b) Coherence of the stacked record with the low field susceptibility from each core. For this calculation, the records have been smoothed to 500 yr. No significant coherence is observed *ca.*  $0.2 \text{ kyr}^{-1}$ . The 95% confidence level is indicated.

is observed differ slightly from core to core but in every case correspond to a insignificant power in the power spectrum. Conversely, no significant coherence is observed *ca.*  $0.2 \text{ kyr}^{-1}$  ( $T = 5 \text{ kyr}$ ) where the power of the stacked record exceeds the 95% confidence level. These results imply that the normalized stack (figure 9) is largely free of environmental/climatic influences and faithfully describes the relative variations of the geomagnetic field in the North Atlantic region.

NAPIS-75 documents that the intensity of the palaeomagnetic field has been highly variable in the last 75 kyr. From 75 ka, the onset of the time-interval considered here, the field strength exhibits some oscillations, with a first minimum at *ca.* 65 ka, followed by a progressive increase to a broad maximum centred at *ca.* 50 ka. There is then an impressive drop to very low values, to a minimum at 40 ka, corresponding to the directional anomaly of the Laschamp event. The duration of the palaeointensity low, about 1500 years as measured by its half-width, is comparable with the estimated duration of the directional change. After recovery, another intensity low observed at *ca.* 34 ka ( $^{14}\text{C}$  dated at *ca.* 28–30 ka corresponding to *ca.* 32–34 ka calendar age (Voelker *et al.* 1998)) corresponds in age to the Mono Lake event (see Liddicoat 1992). After a high at 33 ka and two lows at 30 and 24 ka with a broad maximum between, the field strength seems to slowly increase to the upper limit of the studied interval. Short-lived (millennial-scale) features are superimposed to these trends over the entire interval.

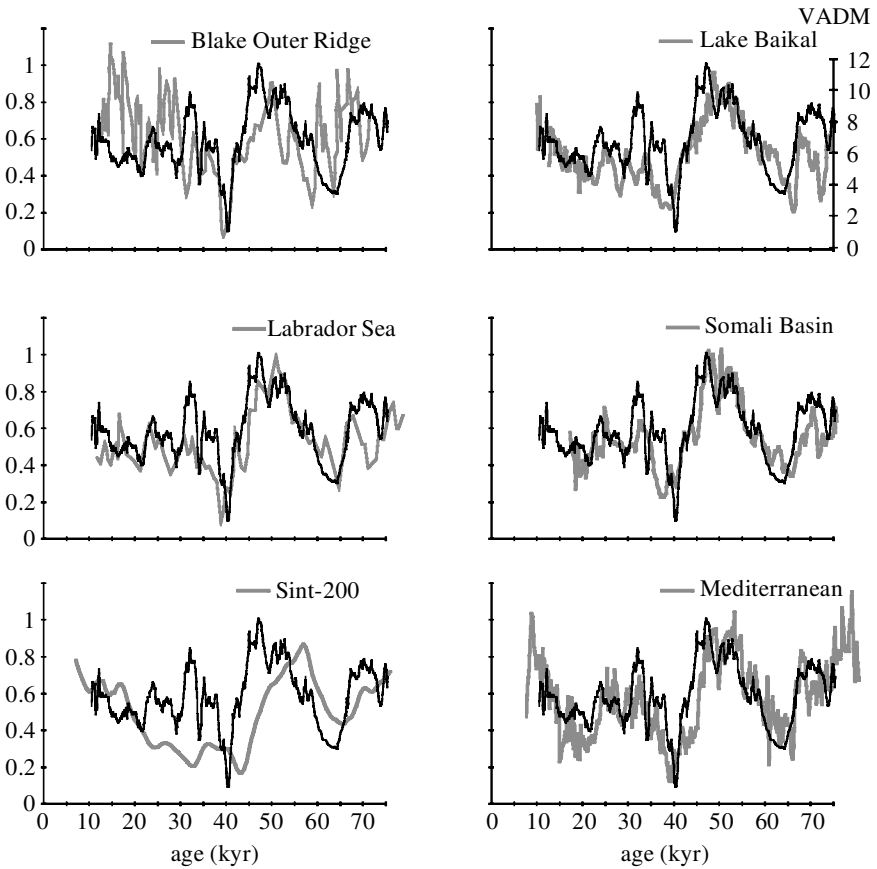


Figure 12. Comparison of NAPIS-75 stack (thicker line) with records obtained from the Blake Outer Ridge (Schwartz *et al.* 1998), Labrador Sea (Stoner *et al.* 1998), Lake Baikal (Peck *et al.* 1996), Somali Basin (Meynadier *et al.* 1992), and Mediterranean Sea (Tric *et al.* 1992), and with Sint-200 (Guyodo & Valet 1996).

(b) Comparison with other records

Figure 12 compares NAPIS-75 with the Sint-200 composite record (Guyodo & Valet 1996), and records obtained from the Labrador Sea (Stoner *et al.* 1998), the Blake Outer Ridge (Schwartz *et al.* 1998), the Lake Baikal (Peck *et al.* 1996), the Mediterranean (Tric *et al.* 1992) and the Somali Basin (Meynadier *et al.* 1992). The long-wavelength trends of geomagnetic field intensity variations, such as the lows *ca.* 40 and 65 ka or the high *ca.* 50 ka, are present in all these records, albeit sometimes at slightly different ages, presumably reflecting inaccuracies in the chronologies of the individual records and/or inconsistencies between age models (NAPIS-75 is placed on the GISP2 age model, while all the other records use marine isotopic ages). However, NAPIS-75 does not exhibit the monotonic increase in intensity documented in the Sint-200 profile for the past 40 kyr. On the contrary, the intensity appears to have been rather stable in the 30–15 ka interval.

The record from core CH88-10P, recently obtained by Schwartz *et al.* (1998) from the Blake Outer Ridge, is similar to NAPIS-75. Some very short-lived features of the

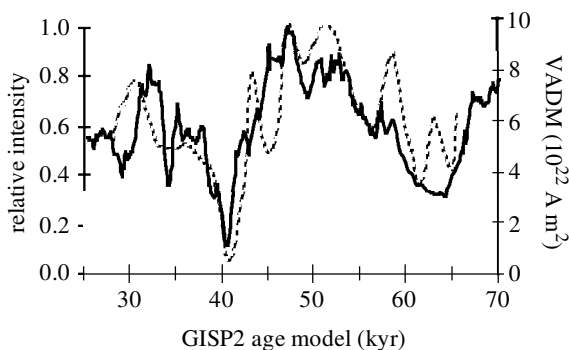


Figure 13. Stacked record NAPIS-75 (continuous line) and VADM record derived from the  $^{36}\text{Cl}$  profile and expressed as VADM (dashed line). The latter is calculated on the basis of the relationship between the  $^{36}\text{Cl}$  production rate and the geomagnetic dipole field intensity (Baumgartner *et al.* 1998). This curve was derived from the measurement of  $^{36}\text{Cl}$  concentrations in the GRIP ice core. It has been low-pass filtered with a cut-off frequency of  $1/3000\text{ yr}^{-1}$  and then transferred to the GISP2 age model (Grootes & Stuiver 1997).

CH88-10P record, however, are not present in NAPIS-75, particularly in the 10–20 ka interval. Striking similarities are observed between NAPIS-75 and the records from the Mediterranean, the Somali Basin and the Lake Baikal, apart from the slightly different age for the 65 ka low in the Somali Basin and Lake Baikal records. Some short-lived features are present in all four records (e.g. in the 30–40 ka interval). The Labrador Sea composite record is also similar to NAPIS-75, both in long-term and short-lived features and its resolution appears to be of the same order as NAPIS-75. Some of the differences between the two records can be attributed to chronological discrepancies between the SPECMAP-derived chronology for the Labrador Sea record (Stoner *et al.* 1998) and the GISP2 chronology for NAPIS-75.

### (c) Comparison with cosmogenic radionuclide production

The strength of the geomagnetic field is the most important factor controlling cosmogenic production. Because shielding of cosmic rays by the geomagnetic field occurs at distances of several Earth radii from the surface, only changes in the dipole field affect shielding. Comparison of cosmogenic flux records is a powerful way of assessing the global (dipolar) nature of the variability of palaeointensity records. Previous work along these lines has shown that  $^{10}\text{Be}$  flux and geomagnetic field intensity anticorrelate in a northern Atlantic core (Robinson *et al.* 1995). In addition, a synthetic reconstruction of palaeointensity, inverted from a global stack of  $^{10}\text{Be}$  marine deposition records, can be correlated to the SINT-200 palaeointensity stack (Franck *et al.* 1997). More recently, it has been demonstrated that the 96–25 ka record of  $^{36}\text{Cl}$  flux from the GRIP ice core agrees quite well with a production-rate calculation based on a palaeointensity stack from the Somali Basin (Baumgartner *et al.* 1998). In figure 13 we compare NAPIS-75 to the synthetic field intensity record calculated from this same  $^{36}\text{Cl}$  record in the 25–65 ka interval, assuming that the variations in the  $^{36}\text{Cl}$  flux are entirely due to modulation by the geomagnetic field. The  $^{36}\text{Cl}$ -derived synthetic palaeointensity profile has been smoothed out using a 3000 year window in order to filter the solar modulation. Originally placed on the GRIP

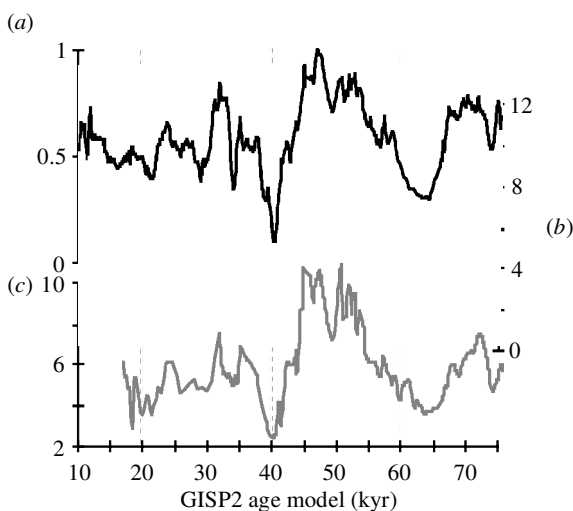


Figure 14. Comparison of the NAPIS-75 record with: (a) the Mediterranean record (Tric *et al.* 1992); (b) the Somali Basin record (Meynadier *et al.* 1992); and (c) after adjusting the time-scales of the Somali and Mediterranean palaeointensity records to maximize the fit to the NAPIS-75 stack.

age model, this profile has been transferred to the GISP2 age model using the results of Grootes & Stuiver (1997). The striking similarities between the observed and synthetic palaeointensity records (figure 13) implies that the NAPIS-75 represents the geomagnetic field, with minimal environmental influence, and that NAPIS-75 reflects the global-scale field, and therefore provides a template for global correlation. We believe that the slight age offsets between NAPIS-75 and the  $^{36}\text{Cl}$ -derived record can be attributed to slight imperfections in the GISP2-GRIP or marine-GISP2 correlations. The coincidence of the maximum in  $^{36}\text{Cl}$  flux (minimum synthetic palaeointensity) with the Laschamp event leaves little doubt that the increase in cosmogenic flux *ca.* 40 ka is due to low geomagnetic field strength, rather than the explosion of a supernova (see Sonnett *et al.* 1987).

(d) *High-resolution chronostratigraphic correlation based on palaeointensity records*

In figure 12, each palaeointensity record is placed on its own independent age model. Assuming the global nature of the NAPIS-75 stack, we adjust the chronologies of the Mediterranean and Somali Basin records by correlation of the palaeointensity records to NAPIS-75. We have chosen the most prominent features as initial tie points, then the small-scale features were adjusted by stretching and/or compressing parts of the Mediterranean and Somali Basin records to maximize their correlation coefficients with NAPIS-75. The maximum stretching/compression corresponds to a shift of about 5000 years from the original age model (this includes the difference between the marine age model and the GISP2 age model used here). After adjustment, the three records can be superimposed (figure 14). The correlation coefficients for the Mediterranean and Somali Basin records are 0.857 and 0.881, respectively, similar to those obtained for the different cores used for constructing NAPIS-75. Using palaeointensity records we have, therefore, achieved the same degree of correla-



tion between North Atlantic and Somali Basin/Mediterranean cores as was obtained within the North Atlantic (to construct NAPIS-75) using more traditional correlation techniques. The correlation coefficients are also similar to those obtained by Peck *et al.* (1996) in the correlation of the Lake Baikal palaeointensity stack with the same Mediterranean and Somali Basin records. Together these results show that millennial-scale variability of palaeointensity records can be used as a global-scale correlation tool. However, it must be stressed that this correlation is certainly limited to particular records. Of the five records which have been compared to NAPIS-75, only two (the Mediterranean and Somali Basin records) covary with NAPIS-75 in fine-scale detail. For other palaeointensity records, either these features do not exist or it is impossible to make unequivocal correlation from core to core. The possibility of obtaining this kind of correlation at millennial scale must, therefore, be considered as exceptional and restricted to cores with high sedimentation rate and uniform magnetic mineralogy.

From a geomagnetic point of view, the presence of coherent short-lived features yields evidence that millennial-scale variability is a fundamental feature of the global-scale (axial dipole) geomagnetic field.

(e) *Duration of the Laschamp event and nature of geomagnetic excursions*

The combination of different factors (precise intercorrelation of the cores, precise correlation to the GISP2 isotopic record, high sediment accumulation rate and uniform mineral magnetic properties) has permitted an estimate for the duration of the Laschamp event (*ca.* 1500 years). This duration estimate is more precise than previous duration estimates for this (or any other) magnetic excursion. It is important to note that the same value is obtained from each of the studied cores, separated by over 5000 km, so that it is not likely that the value is affected by local changes in the sediment deposition rate at the very moment of the geomagnetic event. This determination may have important implications in terms of processes in the Earth's interior. Recently, Gubbins (1999) has proposed that excursions occur when the geomagnetic field reverses in the outer fluid core, which has a typical overturn time of about 500 years, but not in the inner solid core, where diffusion of the field occurs on a typical time-scale of 3000 years. The longer time constant of the inner core delays full reversals of the field, during which time the original polarity may re-establish itself in the outer core, producing an excursion. On the other hand, a full reversal occurs when the field reverses in both the outer and inner cores, and requires a longer time than an excursion. The duration of the Laschamp event determined from NAPIS-75 is 1500 years at most when the GISP2 age model is used. If NAPIS-75 had been placed on a SPECMAP age model, the duration of the intensity low associated with the directional change would be somewhat longer, but in both cases this short duration is inconsistent with a full reversal occurring in the inner core. NAPIS-75 therefore provides supporting evidence for Gubbins's hypothesis of a distinction between excursions and reversals, with the excursions corresponding to processes occurring in the outer core.

## 6. Conclusions

We have obtained a precise record of geomagnetic palaeointensity from the north Atlantic Ocean (NAPIS-75), characterized by high resolution and excellent time con-

tol in the interval 75–10 ka. This record documents a picture of the geomagnetic field with broad trends already recognized in other records and well-resolved short-lived features. By comparison with other palaeointensity records and with the record of  $^{36}\text{Cl}$  in the GRIP ice core we have established the global nature of the variability of NAPIS-75.

A correlation between NAPIS-75 and published records of palaeointensity from the Mediterranean and the Somali Basin obtained by matching long-term trends and short-lived features of the palaeointensity records themselves is obtained with the same accuracy as was achieved in the North Atlantic to construct NAPIS-75 itself using more traditional correlation methods. This underlines the potential of palaeointensity records for high-resolution correlation on a global scale.

The duration of the Laschamp event, which is precisely recorded in five of the cores both in direction and intensity, is about 1500–2000 years. This short duration provides evidence in favour of the hypothesis that excursions correspond to processes in the outer core only, and have a shorter duration than reversals which occur when the field reverses in both outer fluid core and inner solid core.

We express our gratitude to L. Meynadier and J.-P. Valet, J. Peck, M. Schwartz and S. Lund, and J. Stoner for providing us with the numerical data of their palaeointensity records, and to L. Beck, who carried out some of the measurements for core MD95-2034. J. Stoner is also thanked for his careful review of the manuscript. This work has been supported by the French Atomic Energy Commission and the Centre National de la Recherche Scientifique. This is LSCE contribution no. 306.

## References

- Banerjee, S. K., King, J. W. & Marvin, J. 1981 A new method for determination of paleointensity from the ARM properties of rocks. *Earth Planet. Sci. Lett.* **23**, 177–184.
- Bassinot, F. & Labeyrie, L. 1996 Campagne IMAGES MD 101. IFRTP report 96-1.
- Baumgartner, S., Beer, J., Masarik, J., Wagner, G., Meynadier, L. & Synal, H. A. 1998 Geomagnetic modulation of the  $^{36}\text{Cl}$  flux in the GRIP ice core, Greenland. *Science* **279**, 1330–1332.
- Caceci, M. S. 1989 Estimating error limits in parametric curve fitting. *Analyt. Chem.* **61**, 2324–2327.
- Channell, J. E. T., Hodell, D. A. & Lehman, B. 1997 Relative geomagnetic paleointensity and  $\delta^{18}\text{O}$  at ODP Site 983 (Gardar Drift, North Atlantic) since 350 ka. *Earth Planet. Sci. Lett.* **153**, 103–118.
- Day, R., Fuller, M. & Schmidt, V. A. 1977 Hysteresis properties of titano-magnetite: grain-size and compositional dependence. *Phys. Earth Planet. Interiors* **13**, 260–267.
- Franck, M., Schwarz, B., Baumann, S., Kubik, P. W., Suter, M. & Mangini, A. 1997 A 200 kyr record of cosmogenic radionuclide production rate and geomagnetic field intensity from  $^{10}\text{Be}$  in globally stacked deep-sea sediments. *Earth Planet. Sci. Lett.* **149**, 121–129.
- Grootes, P. M. & Stuiver, M. 1997  $^{18}\text{O}/^{16}\text{O}$  variability in Greenland snow and ice with  $10^{-3}$  to  $10^5$  year time resolution. *J. Geophys. Res.* **102**, 26 455–26 470.
- Gubbins, D. 1999 The distinction between geomagnetic excursions and reversals. *Geophys. J. Int.* **137**, F1–F3.
- Guyodo, Y. & Valet, J. P. 1996 Relative variations in geomagnetic intensity from sedimentary records: the past 200 thousand years. *Earth Planet. Sci. Lett.* **143**, 23–26.
- Guyodo, Y. & Valet, J. P. 1999 Global changes in intensity of the Earth's magnetic field during the past 800 kyr. *Nature* **399**, 249–252.
- Hall, P. 1988 Theoretical comparison of bootstrap confidence intervals. *Ann. Stat.* **16**, 927–953.

- King, J. W. & Channell, J. E. T. 1991 Sedimentary magnetism, environmental magnetism and magnetostratigraphy. In *US National Report to International Union of Geodesy and Geophysics. Rev. Geophys. Suppl.*, pp. 358–370.
- King, J. W., Banerjee, S. K., Marvin, J. & Özdemir, Ö. 1982 A new rock-magnetic approach to selecting sediments for geomagnetic paleointensity studies: application to paleointensity for the last 4000 years. *Earth Planet. Sci. Lett.* **59**, 404–419.
- King, J. W., Banerjee, S. K. & Marvin, J. 1983 A comparison of different magnetic methods for determining the relative grain size of magnetite in natural materials: some results from lake sediments. *J. Geophys. Res.* **88**, 5911–5921.
- Kissel, C., Laj, C., Labeyrie, L., Dokken, T., Voelker, A. & Blamart, D. 1999 Rapid climatic variations during marine isotopic stage 3: magnetic analysis of sediments from nordic seas and North Atlantic. *Earth Planet. Sci. Lett.* **171**, 489–502.
- Levi, S. & Banerjee, S. K. 1976 On the possibility of obtaining relative paleointensities from lake sediments. *Earth Planet. Sci. Lett.* **29**, 219–226.
- Liddicoat, J. C. 1992 Mono Lake excursion in Mono Basin, California and at Carson Sink and Pyramid Lake, Nevada. *Geophys. J. Int.* **108**, 442–452.
- Meynadier, L., Valet, J. P., Weeks, R., Shackleton, N. J. & Hagee, V. L. 1992 Relative geomagnetic intensity of the field during the last 140 ka. *Earth Planet. Sci. Lett.* **114**, 39–57.
- Peck, J. A., King, J. W., Colman, S. M. & Kravchinsky, V. A. 1996 An 84 kyr paleomagnetic record from the sediments of Lake Baikal, Siberia. *J. Geophys. Res.* **101**, 11 365–11 385.
- Robinson, C., Raisbeck, G. M., Yiou, F., Lehman, B. & Laj, C. 1995 The relationship between  $^{10}\text{Be}$  and geomagnetic field strength records in central North Atlantic sediments during the last 80 ka. *Earth Planet. Sci. Lett.* **136**, 551–557.
- Schwartz, M., Lund, S. P. & Johnson, T. C. 1998 Geomagnetic field intensity from 71 to 12 ka as recorded in deep-sea sediments of the Blake Outer Ridge, north Atlantic Ocean. *J. Geophys. Res.* **103**, 30 407–30 416.
- Sonnett, C. P., Morfill, C. E. & Jokipii, J. R. 1987 Interstellar shockwaves and  $^{10}\text{Be}$  from ice cores. *Nature* **330**, 458–460.
- Stoner, J. S., Channell, J. E. T. & Hillaire-Marcel, C. 1995 Late Pleistocene relative geomagnetic paleointensity from the deep Labrador Sea: regional and global correlations. *Earth Planet. Sci. Lett.* **134**, 237–252.
- Stoner, J. S., Channell, J. E. T. & Hillaire-Marcel, C. 1998 A 200 kyr geomagnetic chronostratigraphy for the Labrador Sea: indirect correlation of the sediment record to SPECMAP. *Earth Planet. Sci. Lett.* **159**, 165–181.
- Tauxe, L., LaBrecque, J. L., Dodson, R., Fuller, M. & Dematteo, J. 1983 ‘U’ channels—a new technique for paleomagnetic analysis of hydraulic piston cores. *Eos* **64**, 219.
- Tauxe, L., Klystra, N. & Constable, C. 1991 Bootstrap statistics for paleomagnetic data. *J. Geophys. Res.* **96**, 11 723–11 740.
- Tric, E., Valet, J. P., Tucholka, P., Paterne, M., Labeyrie, L., Guichard, F., Tauxe, L. & Fontugne, M. 1992 Paleointensity of the geomagnetic field for the last 80 000 years. *J. Geophys. Res.* **97**, 9337–9351.
- Voelker, A., Sarnhein, M., Grootes, P. M., Erlenkeuser, H., Laj, C., Mazaud, A., Nadeau, M. J. & Schleicher, M. 1998 Correlation of marine  $^{14}\text{C}$  ages from the Nordic sea with GISP2 isotope record: implication for  $^{14}\text{C}$  calibration beyond 25 ka BP. *Radiocarbon* **40**, 517–534.
- Weeks, R., Laj, C., Endignoux, L., Fuller, M., Roberts, A., Manganne, R., Blanchard, E. & Goree, W. 1993 Improvements in long-core measurement techniques: applications in palaeomagnetism and palaeoceanography. *Geophys. J. Int.* **114**, 651–662.